Vascular Platform to Define Hematopoietic Stem Cell Factors and Enhance Regenerative Hematopoiesis

Michael G. Poulos, Michael J.P. Crowley, Michael C. Gutkin, Pradeep Ramalingam, William Schachterle, Jean-Leon Thomas, Olivier Elemento, Jason M. Butler

Stem Cell Reports
Resource
OPEN ACCESS

Vascular Platform to Define Hematopoietic Stem Cell Factors and Enhance Regenerative Hematopoiesis

Michael G. Poulos,[1,2,3] Michael J.P. Crowley,[1,2,3] Michael C. Gutkin,[1,2,3] Pradeep Ramalingam,[1,2,3] William Schachterle,[1,2,3] Jean-Leon Thomas,[4,5,6,7] Olivier Elemento,[8] and Jason M. Butler[1,2,3,*]

[1]Department of Genetic Medicine, Weill Cornell Medical College, New York, NY 10065, USA
[2]Department of Surgery, Weill Cornell Medical College, New York, NY, 10065 USA
[3]Ansary Stem Cell Institute, Department of Medicine, Weill Cornell Medical College, New York, NY 10065, USA
[4]Yale Stem Cell Center, Department of Neurology, Yale University School of Medicine, New Haven, CT 06510, USA
[5]Université Pierre and Marie Curie–Paris 6, 75013 Paris, France
[6]INSERM/CNRS U-1127/UMR-7225, 75013 Paris, France
[7]APHP, Groupe Hospitalier Pitié-Salpètrière, 75013 Paris, France
[8]HRH Prince Alwaleed Bin Talal Bin Abdulaziz Al-Saud Institute for Computational Biomedicine, Weill Cornell Medical College, New York, NY 10065, USA
*Correspondence: jmb2009@med.cornell.edu
http://dx.doi.org/10.1016/j.stemcr.2015.08.018

SUMMARY

Hematopoietic stem cells (HSCs) inhabit distinct microenvironments within the adult bone marrow (BM), which govern the delicate balance between HSC quiescence, self-renewal, and differentiation. Previous reports have proposed that HSCs localize to the vascular niche, comprised of endothelium and tightly associated perivascular cells. Herein, we examine the capacity of BM endothelial cells (BMECs) to support ex vivo and in vivo hematopoiesis. We demonstrate that AKT1-activated BMECs (BMEC-Akt1) have a unique transcription factor/cytokine profile that supports functional HSCs in lieu of complex serum and cytokine supplementation. Additionally, transplantation of BMEC-Akt1 cells enhanced regenerative hematopoiesis following myeloablative irradiation. These data demonstrate that BMEC-Akt1 cultures can be used as a platform for the discovery of pro-HSC factors and justify the utility of BMECs as a cellular therapy. This technical advance may lead to the development of therapies designed to decrease pancytopenias associated with myeloablative regimens used to treat a wide array of disease states.

INTRODUCTION

The adult bone marrow (BM) is composed of distinct microenvironments that maintain hematopoietic stem cell (HSC) homeostasis by modulating self-renewal and differentiation (Morrison and Scadden, 2014). HSCs are located adjacent to the vascular niche, composed of endothelial cells (ECs) and stromal perivascular cells (Kiel et al., 2005; Kunisaki et al., 2013). ECs and LEPR$^+$ mesenchymal stem cells (MSCs) have emerged as primary components of the BM-HSC niche, producing many of the pro-hematopoietic factors needed for HSC homeostasis (Kobayashi et al., 2010; Morrison and Spradling, 2008; Sauvageau et al., 2004). The endothelial and LEPR$^+$ cell-derived cytokines, stem cell factor (KITL) and CXCL12 (SDF1α), are required for the maintenance of the HSC pool (Ding and Morrison, 2013; Ding et al., 2012; Greenbaum et al., 2013). Our group has demonstrated that loss of JAGGED-1 in ECs leads to the premature exhaustion of NOTCH-dependent HSCs (Butler et al., 2010; Poulos et al., 2013). Despite our refined understanding of the architectural and functional communication between the vascular niche and HSCs, the regulatory mechanisms governing these interactions have not been fully elucidated.

Tissue-specific ECs possess distinct gene expression signatures and functional heterogeneity, suggesting that tissue-specific ECs maintain their resident stem cells during homeostasis and regeneration (Nolan et al., 2013). Within the BM microenvironment, perivascular cells found in close association with ECs form an HSC niche, regulating long-term HSC maintenance and quiescence (Kunisaki et al., 2013; Zhou et al., 2014). However, the development of a method to test the ability of niche-specific BM endothelial cells (BMECs) to support repopulating HSCs has been lacking. Moreover, the inability to isolate and cultivate stable, long-lasting, organ-specific murine ECs has limited the field of vascular biology, especially in studies that attempt to define the role of ECs in HSC maintenance. Even when one is able to establish an endothelial culture, the need for chronic supplementation with serum and endothelial-specific growth factors leads to the differentiation of HSCs during co-culture. Current EC isolation protocols result in the cultivation of heterogeneous populations of niche cells, including stromal cells that can rapidly outcompete ECs in long-term cultures.

We have previously demonstrated that AKT1-activated primary human ECs isolated from umbilical vein can expand bona fide mouse HSCs (Butler et al., 2010). In this study, we describe a protocol for the reproducible isolation and culture of AKT1-activated murine BMECs (BMEC-Akt1). Our approach enables the survival of BMEC-Akt1 cultures while maintaining their specific angiogenic and

angiocrine growth factor profiles, without malignant transformation. We have developed a co-culture assay that reveals a dynamic BMEC-Akt1 transcriptional landscape, leading to changes in the BMEC-Akt1 transcription factor and cytokine/growth factor profile in response to hematopoietic cross-talk. BMEC-Akt1 cultures are endowed with the instructive capacity to support long-term repopulating HSCs ex vivo in the absence of complicating exogenous serum and cytokine cocktails. Moreover, the transplantation of niche-specific BMEC-Akt1 cells following an LD_{50} dose of radiation in mice leads to absolute survival and enhances hematopoietic recovery in the absence of a life-saving BM transplant. These mitigating effects were partly achieved by minimizing the duration of pancytopenia and organ damage associated with myeloablative treatment. The establishment of our BMEC-Akt1 cultures will allow us to begin to dissect the complex cellular network of the BM vascular niche by enabling the discrete interrogation of BMEC-HSC interactions, providing a platform to further our understanding of the necessary microenvironmental signals that dictate HSC homeostasis, allowing for the development of tailor-made ex vivo and in vivo therapies for hematological disorders.

RESULTS

Isolation and Characterization of BM Vascular Niche Cells

Using a *Vegfr3::YFP* reporter mouse (Calvo et al., 2011) (Figure 1A), we confirmed that the BM vasculature is composed of two distinct $VECAD^+$ EC populations, including $SCA1^+VEGFR3^-$ arteriole and $SCA1^-VEGFR3^+$ sinusoid ECs (Hooper et al., 2009). To test whether the endothelial and perivascular components of the BM vascular niche support adult HSCs ex vivo, we sought to establish highly pure and robust BMEC and BM stromal (BMS) cultures. Long bones isolated from adult C57BL/6J mice were enzymatically digested and depleted of $lineage^+$ hematopoietic cells, followed by a $CD31^+$ cell enrichment. $CD31^+$ and $CD31^-$ cell suspensions were plated on fibronectin-coated wells and transduced with a constitutively active *Akt1*-expressing lentivirus, allowing for the outgrowth of primary $CD31^+$ BMECs (BMEC-Akt1) and $CD31^-$ BMS (BMS-Akt1) (Figure 1A). Resulting cultures expressed genes characteristic of endothelial and stromal cells (Figures S1A and S1B). To confirm the identity of our BMEC-Akt1 cultures, we analyzed the expression of pan EC (VECAD), arteriole EC (SCA1), and sinusoidal EC (VEGFR3) markers (Hooper et al., 2009). BM-derived ECs displayed a phenotypic arteriole identity, staining for SCA1, but not VEGFR3 (Figure 1B). To test the ability of our BMEC-Akt1 cultures to undergo in vivo tubulogenesis, matrigel plugs containing mCherry-labeled BMEC-Akt1 and mCerulean-labeled BMS-Akt1 cells were implanted subcutaneously into C57BL/6J mice and assayed for vessel formation and anastomosis. Matrigel plugs revealed co-localization of $mCherry^+$ cells with an Isolectin-B_4 intravital vascular label (Figure 1C), while BMS-Akt1 controls were found within the interstitial parenchymal space. BMS-Akt1 cells expressed PDGFRA, LEPR, and PRX1 (Figure 1D), suggesting that our stromal cultures contain $LEPR^+$ perivascular niche cells that contribute to the maintenance of HSCs in vivo (Ding and Morrison, 2013; Ding et al., 2012). Given that $LEPR^+$ stromal cells possess features of MSCs (Zhou et al., 2014), we analyzed the potential of our isolated stromal cells to differentiate into MSC lineages. BMS-Akt1 cells were able to form osteoblasts, chondrocytes, and adipocytes in in vitro differentiation assays, staining positively for Alizarin Red S (osteoblast), Oil Red O (adipocyte), and Toluidine Blue O (chondrocyte) (Figure 1E). Differentiated BMS-Akt1 cells also upregulated tissue-specific transcripts, including *Bglap*, *Omd* (osteoblast), *Fasn*, *Acly* (adipocyte), *Acan*, *Hapln1* (chondrocyte) (Figure S1C).

Whole-transcriptome profiling (RNA sequencing) of BMEC-Akt1 and BMS-Akt1 cultures confirmed enrichment of arteriole EC and canonical MSC-related genes (Figures 2A and 2B). BMEC-Akt1 and BMS-Akt1 cells were also enriched for pro-hematopoietic growth factors (Figures 2A and 2B) expressed in the in vivo BM endothelial and stromal microenvironment (Figure S2). Gene ontology (GO) analysis demonstrated that differentially expressed genes in BMEC-Akt1, compared with BMS-Akt1, were associated with blood vessel development, while differentially expressed genes in BMS-Akt1 cells were enriched for processes that maintain the structure and function of tissues (Figures 2C and 2D). Taken together, we have isolated robust, long-term BMEC-Akt1 and BMS-Akt1 cultures that maintain their functional capacities. Isolated BMEC-Akt1 and BMS-Akt1 cells demonstrated the ability to be cultured for at least 14 days without serum or exogenous cytokines (data not shown); we next sought to examine the instructive capacity of BMEC-Akt1 and BMS-Akt1 cells in serum- and cytokine-free hematopoietic stem and progenitor cell (HSPC) co-cultures to support long-term repopulating HSCs.

BMEC-Akt1 Supports the Ex Vivo Culture of Repopulating HSCs

To examine the capacity of our BMEC-Akt1 and BMS-Akt1 cells to support HSCs, we developed an ex vivo co-culture system in which $CD45^+lineage^-cKIT^+SCA1^+$ (LKS) HSPCs were cultured on a feeder layer of BMEC-Akt1 or BMS-Akt1 cells under serum-free conditions. Adult C57BL/6J ($CD45.2^+$) HSPCs were sorted to purity and plated (2,500 LKS cells) on a confluent well of BMEC-Akt1 or BMS-Akt1 cells in StemSpan Serum-Free media supplemented with

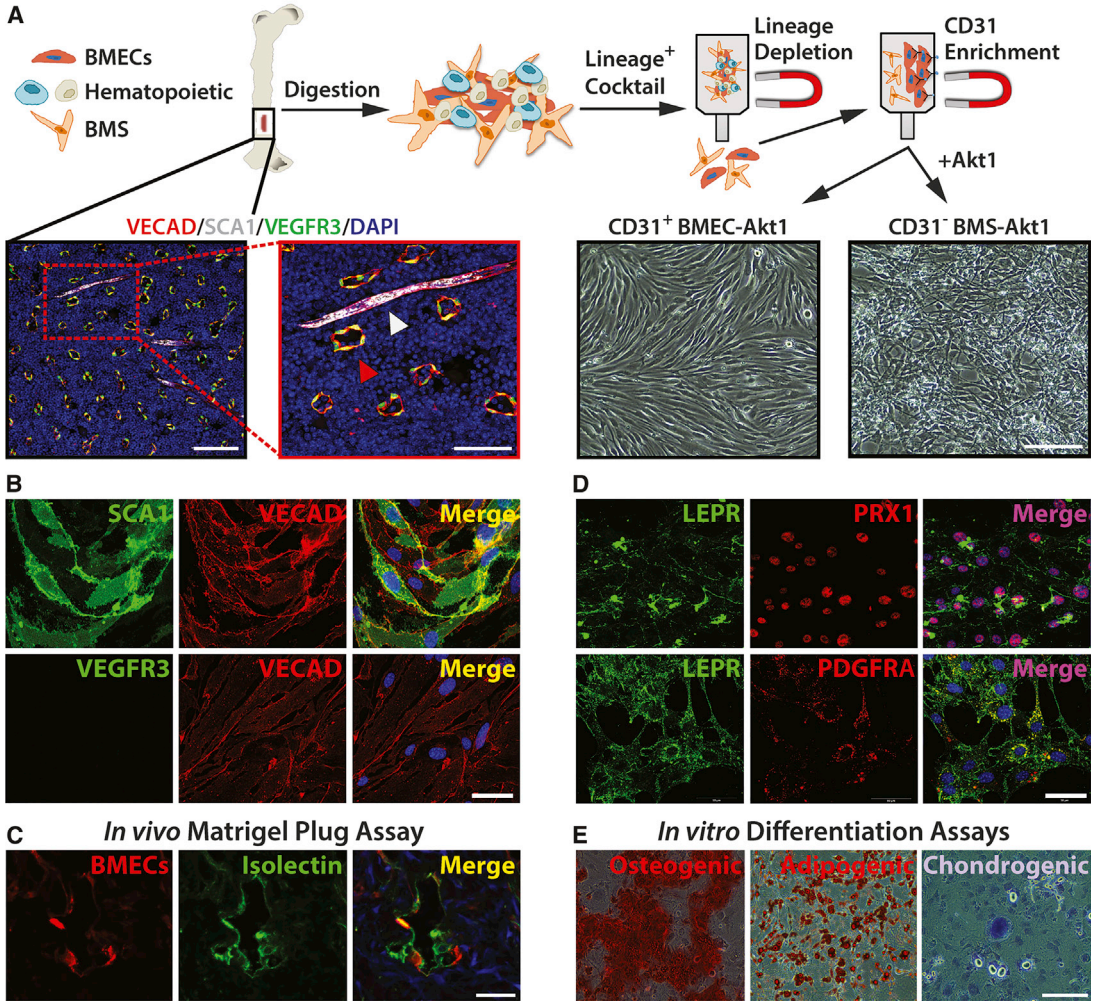

Figure 1. Generation of BM-Derived Endothelial and Stromal Cells

(A) Schematic of BMEC and BMS cell isolations. VECAD$^+$SCA1$^+$VEGFR3$^-$ arteriole (white arrowhead) and VECAD$^+$SCA1$^-$VEGFR3$^+$ sinusoidal (red arrowhead) BMECs in vivo (scale bar represents 100 and 50 μm). Phase-contrast images of isolated BMEC-Akt1 and BMS-Akt1 cultures (scale bar represents 200 μm).

(B and C) BMEC-Akt1 cultures demonstrate VECAD$^+$SCA1$^+$VEGFR3$^-$ arteriole staining (B) (scale bar represents 50 μm) and produce vessels in vivo (C). BMEC-Akt1 (red), but not BMS-Akt1 (blue), co-localize with intravitally labeled vasculature (Isolectin-B_4; green) in matrigel plugs (scale bar represents 25 μm).

(D and E) BMS-Akt1 cultures display PDGFRA$^+$PRX1$^+$LEPR$^+$ BMS staining (D) (scale bar represents 50 μm) and give rise to osteogenic (Alizarin Red S), adipogenic (Oil Red O), and chondrogenic (Toluidine Blue O) progeny in vitro (E) (scale bar represents 200 μm).

50-ng/ml soluble KITL (sKITL). No feeder cultures served as controls (Figures 3A and 3B). Hematopoietic cells were assayed following 9 days of co-culture. While BMEC-Akt1 and BMS-Akt1 promoted the expansion of total CD45$^+$ cells, only BMEC-Akt1 supported the expansion of phenotypic HSPCs (greater than >14-fold), with no feeder and BMS-Akt1 conditions unable to maintain input levels of phenotypic LKS cells (Figures 3C and S3). Lineage$^+$ cells were primarily phenotypic GR1$^+$/CD11B$^+$ myeloid for all co-culture conditions (data not shown). To quantify progenitor activity, total CD45$^+$ cells were sorted from BMEC-Akt1 and BMS-Akt1 co-cultures, plated in methylcellulose, and scored for colony-forming units (CFUs). All conditions maintained appreciable levels of progenitor activity, while BMEC-Akt1 co-cultured CD45$^+$ cells possessed significantly higher levels of CFU-E and CFU-G activity (Figures 3D and 3E). To assess the long-term, multi-lineage engraftment capacity of our ex vivo co-cultured HSPCs, 10^5 total CD45.2$^+$ sorted cells were transplanted into lethally irradiated (950 Rads) CD45.1$^+$ recipients with 5 × 10^5 CD45.1$^+$ whole BM (WBM) cells as a competitive dose. BMEC-Akt1 co-cultured CD45$^+$ cells show stable engraftment in recipient

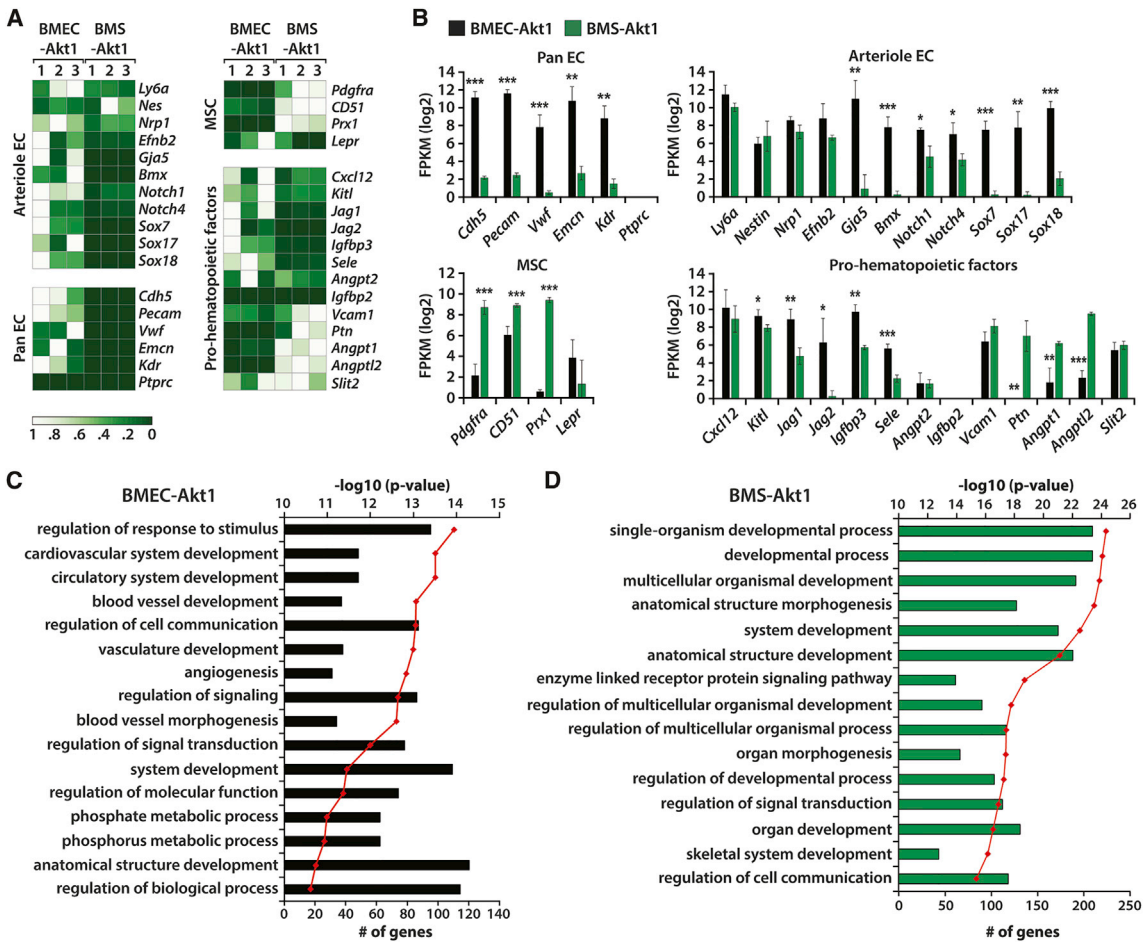

Figure 2. BMEC-Akt1 and BMS-Akt1 Cells Express Pro-hematopoietic Factors and Are Enriched in Pathways Involved in Vascular and Organ Development

(A) Heatmaps of relative gene expression from three independently derived BMEC-Akt1 and BMS-Akt1 lines.

(B) BMEC-Akt1 and BMS-Akt1 cultures demonstrate enrichment in endothelial and MSC gene expression, respectively. BMEC-Akt1 and BMS-Akt1 cultures show enrichment for pro-hematopoietic factors. Error bars represent mean ± SEM and significance was determined by Student's t test; *$p < 0.05$, **$p < 0.01$, ***$p < 0.001$. Three independently isolated BMEC-Akt1 and BMS-Akt1 lines were analyzed.

(C and D) BMEC-Akt1 lines are enriched in angiogenic and vascular development pathways. GO analysis of differentially expressed genes in BMEC-Akt1 and BMS-Akt1 cell lines reveals the enrichment of distinct pathways ($-\log_{10}$ p value = red line; number of genes enriched in target pathway = bar graph).

mice (Figures 3D and 3F), with BMS-Akt1 and feeder-free controls producing diminutive levels of CD45.2$^+$ cells in the peripheral blood. BMEC-Akt1 co-cultured CD45.2$^+$ cells were capable of multilineage engraftment at 16 weeks (Figure 3G), while BMS-Akt1 and no feeder CD45.2$^+$ controls did not make significant contributions to any lineage (data not shown). To test the self-renewal capability of the BMEC-Akt1 co-cultured CD45.2$^+$ HSCs and eliminate the possibility that co-cultures enriched for progenitor activity promoted primary hematopoietic engraftment, we performed secondary transplantations and found an increase in the percentage of engrafted CD45.2$^+$ cells at 16-weeks post-transplant with multilineage potential (Figure 3H). These data suggest that BMEC-Akt1 acts as an ex vivo pro-HSC niche that provides the appropriate combination and levels of angiocrine factors that regulate the maintenance of HSCs, retaining their ability to repopulate lethally irradiated recipients, leading to long-term, multilineage engraftment.

BMEC-Akt1 Co-cultures Support HSCs without Exogenous KITL

Genetic evidence indicates that the deletion of *Kitl* in ECs results in a significant decrease in overall HSC numbers and function in the BM (Ding et al., 2012). To test whether cultured BMEC-Akt1 express physiological levels of KITL

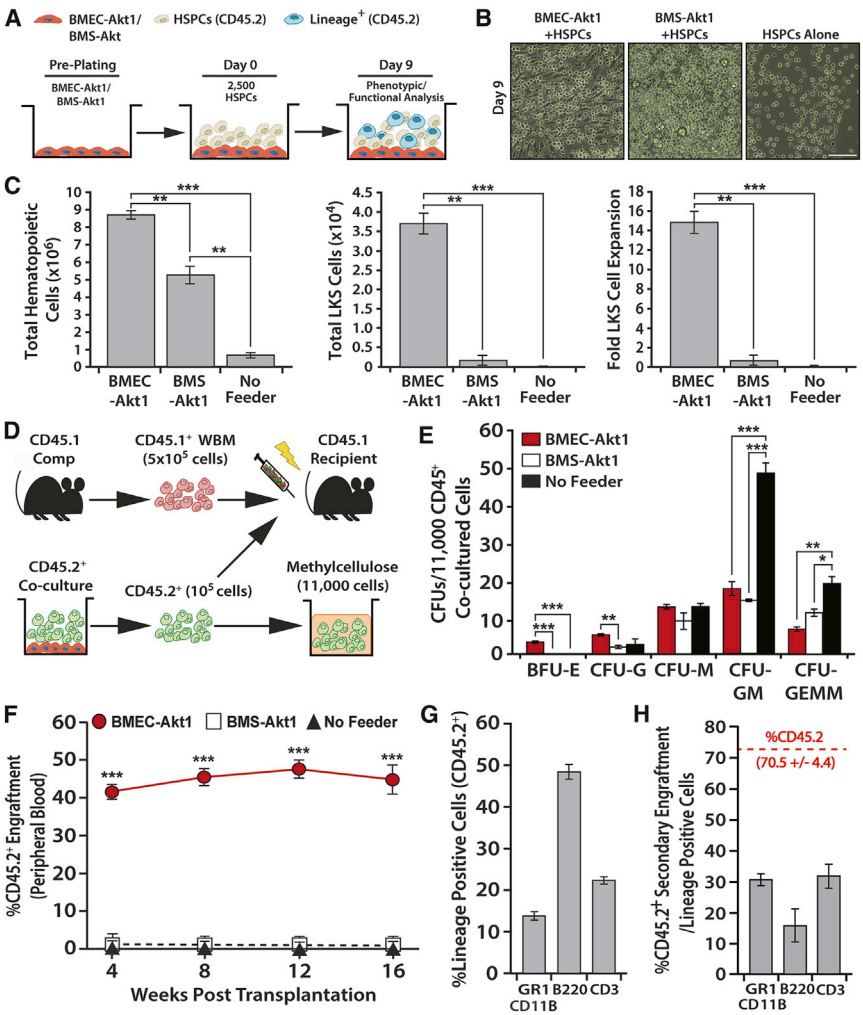

Figure 3. BMEC-Akt1 Cultures Support HSPCs under Serum-Free Conditions Ex Vivo

(A) Schematic of ex vivo co-culture assay. HSPCs were co-cultured for 9 days with 50-ng/ml sKITL in serum-free media.

(B) Phase-contrast images of day 9 HSPC co-cultures (scale bar represents 200 μm).

(C) BMEC-Akt1 cells support HSPC maintenance ex vivo. Quantification of total CD45$^+$ hematopoietic cells and LKS HSPCs following 9 days of co-culture. Fold expansion is defined as total LKS (day 9)/input LKS (day 0).

(D) Schematic of functional assays. Day 9 co-cultured CD45.2$^+$ cells were purified from feeders and plated in methylcellulose and scored for CFUs or transplanted into lethally irradiated CD45.1$^+$ recipients with a CD45.1$^+$ WBM competitive dose.

(E) BMEC-Akt1 co-cultures maintain multilineage hematopoietic progenitor activity ex vivo.

(F and G) HSPCs cultured on BMEC-Akt1 cells engraft lethally irradiated recipients (F) and demonstrate multilineage potential 16 weeks post-transplant (G).

(H) BMEC-Akt1 cultured HSCs engraft secondary recipients (dashed red line) and maintain multilineage potential. n = 10 mice per condition. Error bars represent mean ± SEM and significance was determined by Student's t test; *p < 0.05, **p < 0.01, ***p < 0.001.

that support the maintenance of repopulating HSPCs ex vivo, we co-cultured HSPCs on BMEC-Akt1 in the absence of exogenous sKITL. Omitting sKITL resulted in a significant decrease in total hematopoietic cells and HSPC fold expansion (Figures 4A and 4B). However, even in the absence of exogenous sKITL, BMEC-Akt1 cultures were still able to expand phenotypic LKS HSPCs by 3.5-fold (Figure 4A). Total CD45$^+$ cells co-cultured in the presence or absence of exogenous sKITL displayed no differences in progenitor activity (Figure 4C). To assess long-term engraftment, 10^5 CD45.2$^+$ co-cultured cells and 5×10^5 CD45.1$^+$ competitor WBM cells were transplanted into lethally irradiated CD45.1$^+$ recipients. BMEC-Akt1 co-cultured HSPCs without sKITL (Figure 4D; black box, solid line) were able to produce long-term engraftment, albeit at a significantly lower proportion than cultures supplemented with sKITL (Figure 4D; red circle, solid line). To confirm that BMEC-Akt1 cultures were supporting long-term repopulating HSCs, we transplanted 1000 CD45.2$^+$ LKS cells from co-cultures without sKITL with 5×10^5 short-term CD45.1$^+$ Sca1-depleted WBM into lethally irradiated CD45.1$^+$ mice. CD45.2$^+$ HSPCs cultured on BMEC-Akt1 in the absence of sKITL resulted in long-term engraftment that stabilized at >90% by 16-weeks post-transplant (Figure 4D; black box, dashed line), with myeloid and lymphoid contributions similar to non-competitive transplantations (Figure 4E). These data suggest that BMEC-Akt1 provides sufficient angiocrine signals to promote the maintenance of bona fide HSCs ex vivo.

HSPC Co-culture Modulates BMEC-Akt1 Gene Expression

In the BM microenvironment, HSCs are found in close proximity to the vasculature (Kiel et al., 2005; Kunisaki et al., 2013), suggesting that direct cellular contact may be necessary for the maintenance of resident stem cells. However, little is known about the cross-talk between HSCs and cells that composes the supportive environment.

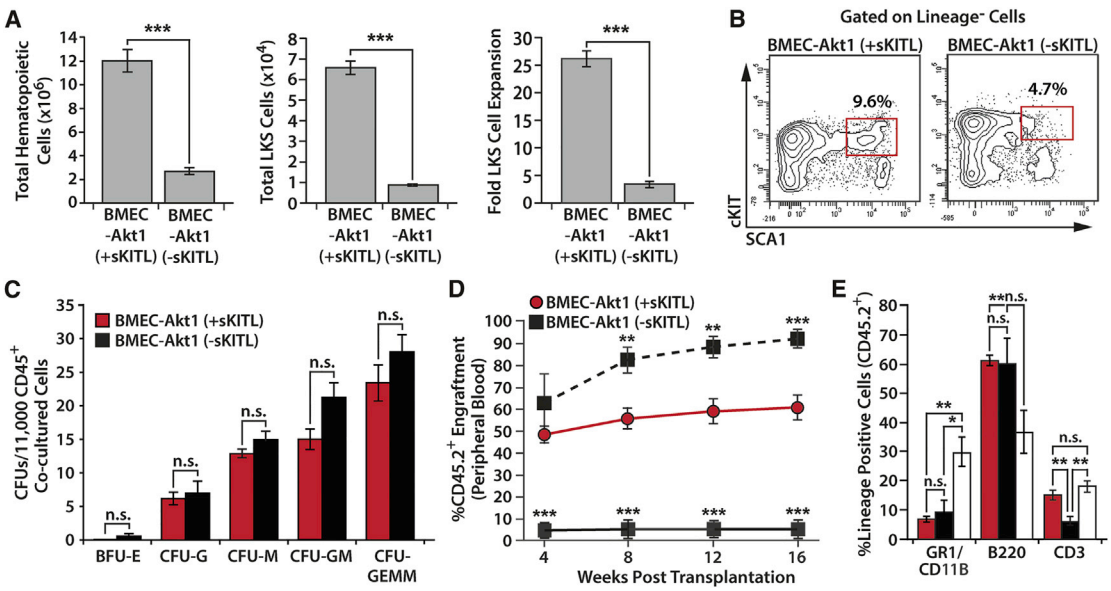

Figure 4. BMEC-Akt1 Support HSPCs Ex Vivo in the Absence of Exogenous Cytokines

(A) BMEC-Akt1 cells without sKITL maintain HSPCs ex vivo. Quantification of total CD45$^+$ hematopoietic cells and LKS HSPCs following 9 days of co-culture in serum-free conditions. Fold expansion is defined as total LKS (day 9)/input LKS (day 0).

(B) Representative contour plots of expanded LKS cells. Plots are gated on lineage$^-$ populations (not shown). Frequency of cKIT$^+$SCA1$^+$ populations (red box) are expressed as a percentage of total lineage$^-$ cells.

(C) sKITL is not required to maintain multi-lineage hematopoietic progenitor activity. CFUs were assayed from total CD45$^+$ cells following co-culture.

(D) BMEC-Akt1 maintain long-term repopulating HSCs in the absence of serum and exogenous cytokines. Total CD45.2$^+$ cells co-cultured on BMEC-Akt1 −sKITL (red circle, solid line) or +sKITL (black square, solid line) were transplanted with a standard CD45.1$^+$ WBM rescue dose. Purified LKS cells from BMEC-Akt1 HSPC co-cultures-sKITL (black box, dashed line) were transplanted with a CD45.1$^+$ SCA1-depleted WBM rescue dose. Engraftment was monitored by %CD45.2$^+$ contribution to the peripheral blood.

(E) BMEC-Akt1 +sKITL (red), BMEC-Akt1 -sKITL (black), and BMEC-Akt1 -sKITL with Sca1-depleted rescue dose (white) co-cultures demonstrated multilineage engraftment at 16-weeks post-transplant. n = 10 mice per condition. Error bars represent mean ± SEM, and significance was determined by Student's t test. *p < 0.05, **p < 0.01, ***p < 0.001, n.s., not significant.

To explore this reciprocal cross-talk, we co-cultured BMEC-Akt1 and BMS-Akt1 with HSPCs (Figure 3A), sorted (CD45$^-$DAPI$^-$) to collect purified feeders (Figure S4), and analyzed via RNA sequencing. Feeders grown in co-culture media without HSPCs were used as baseline controls. Principal component analysis (PCA) and hierarchical clustering of RNA-sequencing data from cultured BMEC-Akt1 and BMS-Akt1 cells alone or following co-culture demonstrated a strong segregation into four distinct groups, accounting for 90% of the variance in the dataset (Figures 5A and S4B). Pairwise comparisons of BMEC-Akt1 ± HSPCs and BMS-Akt1 ± HSPCs co-cultured feeders yielded 184 and 270 differentially expressed genes, respectively (Figures 5B–5D). The distribution and significance of gene expression is visualized by comparing the $\log_2$ fold change with the $-\log_{10}$ p value and by scaling the $\log_2$ FPKM values by row in a heatmap (Figures 5C and 5D). Analysis of pro-hematopoietic factors revealed a similar pattern of expression for most genes in the individual cell type and co-cultures (Figure 5E). Nine differentially expressed transcription factors were observed in BMEC-Akt1, four of which were upregulated (*Myb*, *Nfe2*, *Sox9*, and *Vdr*) and five of which were downregulated (*Egr3*, *Esr1*, *Fosb*, *Id4*, and *Tox2*) in the presence of HSPCs (Figure 5F, left). Twelve transcription factors were differentially expressed in the BMS-Akt1 cells, ten of which were upregulated (*Atf3*, *Bhlhe40*, *Fosb*, *Jun*, *Junb*, *Jund*, *Klf2*, *Klf4*, *Maff*, and *Nfil3*) and two of which were downregulated (*Lhx6* and *Nr4a2*) following co-culture (Figure 5F, right). *Fosb* was common between these two lists; however, it was differentially regulated between BMEC-Akt1 and BMS-Akt1 in the presence of HSPCs. Nine and seven differentially expressed cytokines were identified in BMEC-Akt1 and BMS-Akt1 cell lines, respectively (Figure 5G); BMEC-Akt1 co-cultures upregulated the expression of eight genes (*Ccl7*, *Ccl9*, *Ccr2*, *Lrg1*, *Pf4*, *Pglyrp1*, *Ppbp*, and *Tnfrsf9*) and downregulated the expression of one gene (*Cx3cl1*) and BMS-Akt1 co-cultures upregulated the expression of three genes (*Gpi1*, *Itgb3*, and

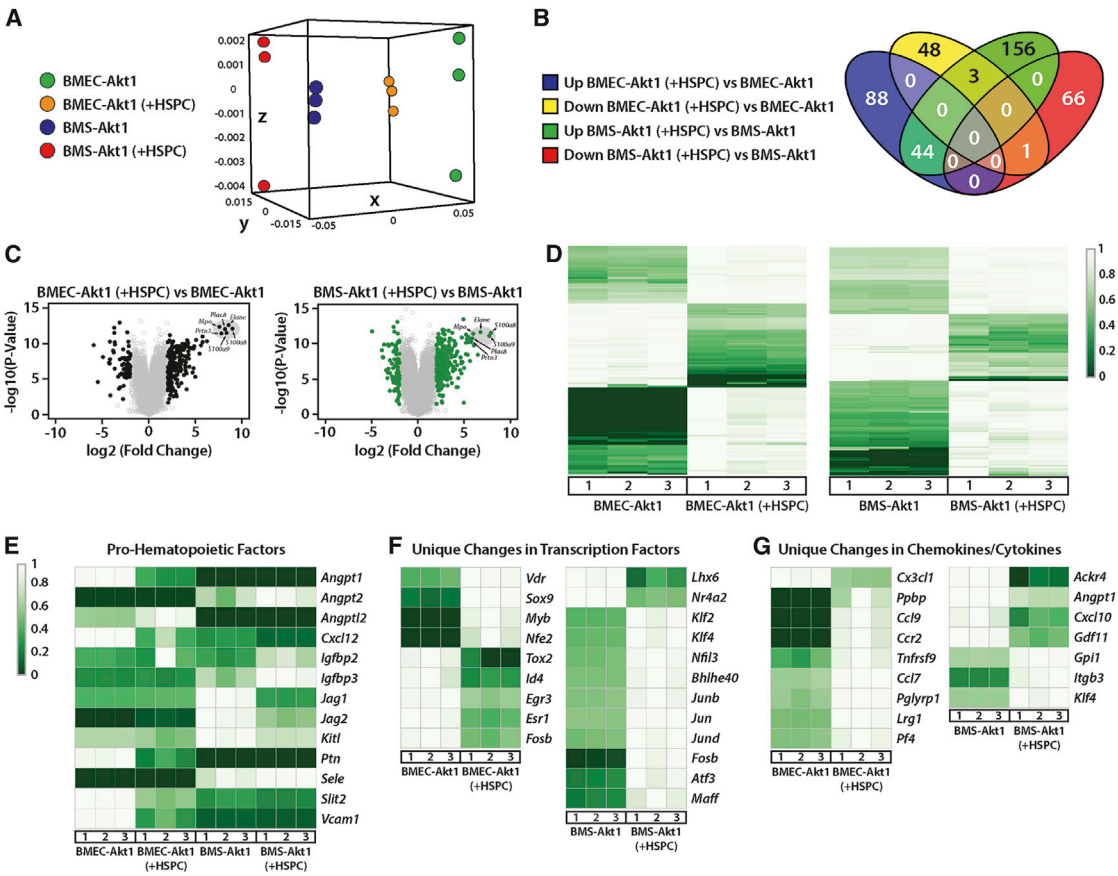

Figure 5. HSPCs Modulate Gene Expression Changes in BMEC-Akt1 and BMS-Akt1 Cells

(A) PCA of BMEC-Akt1 and BMS-Akt1 cell lines alone and in co-culture with HSPCs.

(B) Venn diagram of differentially expressed (absolute $\log_2$ fold change > 2, p value < 0.05, and expression >10 FPKM) genes in the BMEC-Akt1 ± HSPC and BMS-Akt1 ± co-culture comparisons.

(C and D) Distributions of gene expression were visualized by volcano plots of the $\log_2$ fold change and $-\log_{10}$ p values and heatmaps of BMEC-Akt1 and BMS-Akt1 cells alone or following HSPC co-culture. Differentially expressed genes (absolute $\log_2$ fold change > 2, p value < 0.05) are marked as black and green for BMEC-Akt1 and BMS-Akt1, respectively. Representative conserved gene expression changes are noted.

(E) Heatmaps of known pro-hematopoietic factors following HSPC co-culture.

(F and G) Differentially expressed transcription factors (F) and chemokines and cytokines identified in BMEC-Akt1 and BMS-Akt1 cell lines following co-culture with HSPCs (G). Three independently isolated BMEC-Akt1 and BMS-Akt1 cell lines were analyzed.

Klf4) and downregulated the expression of four genes (*Ackr4*, *Angpt1*, *Cxcl10*, and *Gdf11*). These data demonstrate that reciprocal cross-talk occurs between HSPCs and the supporting feeder cells and provide a platform to elucidate and test paracrine factors that can modulate the maintenance of repopulating HSCs ex vivo.

Transplantation of BMEC-Akt1 Promotes Hematopoietic Regeneration

Long-term survival of many hematological diseases requires radiation and/or chemotherapy to induce remission. One underappreciated mechanism that can account for the deleterious effects of this therapy in patients is that the irreversible damage radiological or chemotherapeutic insult may cause to the BM microenvironment. Because the vascular niche is critical for recovery of the hematopoietic compartment and maintain HSCs ex vivo, we tested whether transplantation of healthy niche-specific BMEC-Akt1 cells could improve hematopoietic recovery following insult. C57BL/6J mice were subjected to 700 Rads of total body irradiation (TBI), corresponding to an LD_{50} myeloablative dose, and transplanted with either 5×10^5 BMEC-Akt1, 5×10^5 BMS-Akt1, or PBS (control) on 4 successive days. Hematopoietic recovery of peripheral blood was assessed every 7 days, and survival was monitored for 28 days post-irradiation, at which time mice were sacrificed and assayed for total

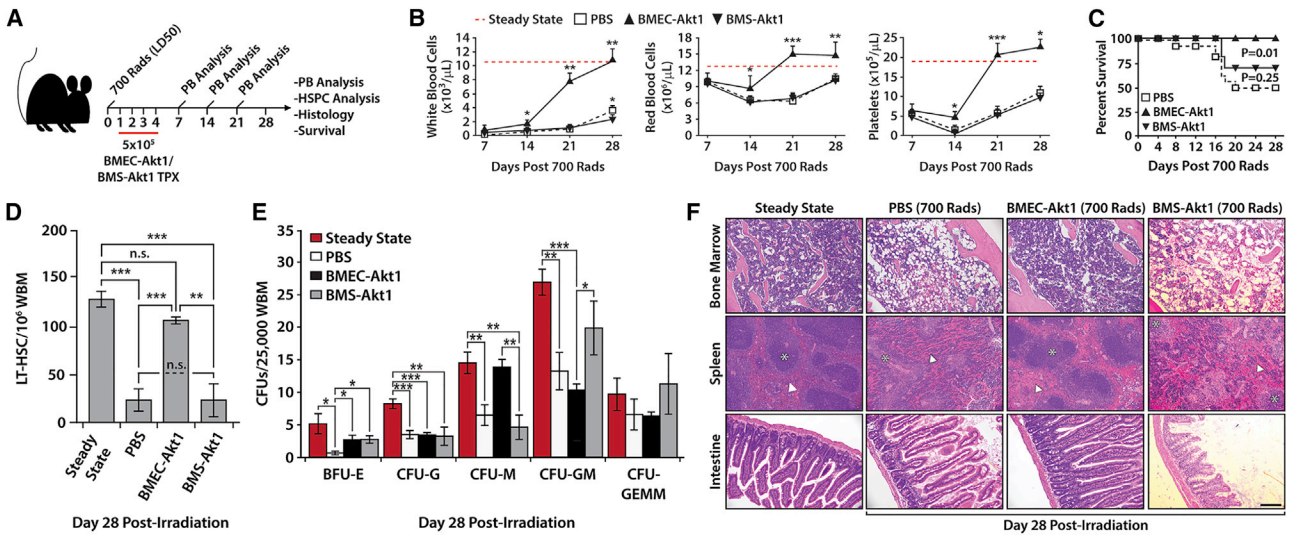

Figure 6. Transplantation of BMEC-Akt1 Promotes Survival and Rapid Hematopoietic Recovery Following Myeloablation

(A) C57BL/6J mice were subjected to an LD_{50} dose of TBI (700 Rads), transplanted on four successive days post-irradiation with either 5×10^5 BMEC-Akt1, 5×10^5 BMS-Akt1, or PBS control and assayed for hematopoietic recovery.

(B) BMEC-Akt1, but not BMS-Akt1 transplantation, expedites peripheral hematopoietic recovery.

(C) BMEC-Akt1 transplantation, but not BMS-Akt1 or PBS controls, absolutely mitigate radiation-induced death.

(D) BMEC-Akt1 transplantations protect phenotypic LT-HSCs. LT-HSCs were quantified from WBM using LKS and $CD150^+CD48^-$ markers.

(E) Hematopoietic progenitor activity in BMEC-Akt1, BMS-Akt1, and PBS transplanted mice. CFUs were assayed from $CD45^+$ WBM at day 28 post-irradiation.

(F) H&E-stained BM (trabecular region-femur) show cytopenia 28 days post-irradiation in BMS-Akt1 and PBS control mice, while BMEC-Akt1 transplantations display marked recovery. The spleen, including both red (asterisk) and white pulp (arrowhead), and intestine also demonstrate preserved tissue morphology. n = 10 mice per cell transplant; n = 20 mice per PBS transplant. Error bars mean ± SEM and significance was determined by Student's t test; *p < 0.05, **p < 0.01, ***p < 0.001. Survival curve probability was determined using the log-rank test.

LT-HSC recovery, hematopoietic progenitor activity, and tissue morphology (Figure 6A). Mice transplanted with BMEC-Akt1 displayed a rapid recovery of total white blood cells, red blood cells, and platelets in the peripheral blood, with significant gains as early as 14-days post-irradiation and a return to steady-state levels by day 21 (Figure 6B), while surviving BMS-Akt1 and PBS injected mice were in active recovery at day 28. BMEC-Akt1 cells completely mitigated radiation-induced hematopoietic failure and death, independent of a BM transplant, suggesting a tempering of radiation-induced hematopoietic cell damage or reestablishment of a functional BM microenvironment (Figure 6C). BMS-Akt1 transplantation partially mitigated radiation-induced death, but was not significantly different when compared with PBS controls. BMEC-Akt1 transplants also demonstrated an increase in the frequency of phenotypic LT-HSCs (Figure 6D). While transplantation of both BMEC-Akt1 and BMS-Akt1 maintained appreciable levels of progenitor activity, only CFU-M and CFU-GM significantly differed between cell types (Figure 6E). Histology of the trabecular region of the femur BMEC-Akt1 transplantation demonstrated a striking radio-protective effect when compared to BMS-Akt1 and PBS controls, with little observable BM hypocellularity associated with myeloablation (Figure 6F). BMEC-Akt1 transplantation also had a profound effect on the morphology of the spleen following TBI, which displayed normal architecture, including localized red and white pulp (Figure 6F). BMEC-Akt1 transplants also showed a distinct preservation of another radiosensitive tissue, the intestine (Figure 6F). These data demonstrate that transplantation of BMEC-Akt1, but not BMS-Akt1, results in a protective effect that mitigates deleterious consequences associated with TBI.

To examine the possibility that soluble factors produced by BMEC-Akt1 are promoting hematopoietic recovery following myeloablation, BMEC-Akt1 conditioned media were administered to C57BL/6J mice following 700 Rads of TBI, and hematopoietic recovery was monitored for 28-days post-irradiation (Figure S5A). BMEC-Akt1 transplanted mice displayed more efficient peripheral white blood cell, red blood cell, and platelet recovery compared with conditioned media (Figure S5B). While both BMEC-Akt1 transplanted and conditioned media infused mice displayed a reduction in mortality, BMEC-Akt1 mice displayed

complete survival and conditioned media demonstrated an incomplete attenuation of radiation-induced death (Figure S5C). Mice transplanted with BMEC-Akt1, but not conditioned media, demonstrated an increase in the frequency of phenotypic LT-HSCs (Figure S5D), with no observable changes in progenitor activity (Figure S5E). Conditioned media failed to protect radiosensitive tissues, when compared with BMEC-Akt1 controls (Figure S5F).

BMEC-Akt1 Do Not Engraft Tissues Following Myeloablative Transplantation

To determine whether BMEC-Akt1 radioprotection was mediated by vascular engraftment, we examined tissues and peripheral blood at short- and long-term time points following an LD_{50} dose of TBI following transplantation of mCherry-labeled BMEC-Akt1 (derived from CD45.2$^+$ mice) into syngeneic CD45.1$^+$ recipients (Figure S6A). Unlabeled CD45.2$^+$ WBM transplantations were used as controls. mCherry$^+$ BMEC-Akt1 cells were present in the peripheral blood at days 4 and 7 post-irradiation (Figure S6B), but were undetectable at day 14 and 16 weeks (Figures S6B and S6D). The absence of detectable CD45.2$^+$ hematopoietic cells in mCherry-BMEC-Akt1 transplanted mice at short- and long-term time points confirms that hematopoietic recovery is independent of contaminating hematopoietic cells in our cultures (Figures S6C and S6D). To assess tissue-specific BMEC-Akt1 engraftment, transplanted mice were intravitally labeled with Isolectin-B_4 prior to sacrifice and assayed by immunohistochemistry (IHC) at short- and long-term time points. mCherry$^+$ BMEC-Akt1 were present within the BM at early time points, but were absent at 16-weeks post-irradiation (Figure S6E). mCherry$^+$ BMEC-Akt1 cells were not observed in the spleen at either short- or long-term time points (Figure S6F). mCherry$^+$ BMEC-Akt1 cells were also undetectable within the BM microenvironment by flow cytometry at 16 weeks (data not shown). Therefore, BMEC-Akt1 are transiently present following myeloablative injury, but do not engraft tissues long-term, consistent with other reports (Chute et al., 2007; Li et al., 2010; Salter et al., 2009). These data suggest that transplanted BMEC-Akt1 exerts its pro-regenerative effects rapidly and transiently.

Niche-Specific ECs Promote Efficient Hematopoietic Recovery

Each organ is endowed with specialized endothelium that has a unique angiocrine signature that may support their resident stem cells (Nolan et al., 2013). Tissue-specific ECs can enhance organ regeneration, while non-resident ECs are unable to elicit the same regenerative effect (Ding et al., 2010, 2011). To test this, 5×10^5 niche-specific BMEC-Akt cells or non-hematopoietic pulmonary artery ECs, brain microvascular ECs, or secondary-hematopoietic BM endothelial progenitor cells (BM EPCs) were transplanted into C57BL/6J mice following an LD_{50} dose of TBI (Figure 7A). While all EC transplants prevented radiation-induced death (Figure 7C), mice transplanted with BMEC-Akt1 displayed an accelerated recovery of white blood cells, red blood cells, and platelets in the peripheral blood (Figure 7B). BMEC-Akt1 transplantations demonstrate more phenotypic LT-HSCs than lung EC and PBS controls, but brain and BM EPC transplantations displayed higher phenotypic LT-HSCs when compared with BMEC-Akt1 (Figure 7D). However, representative LKS CD150$^+$CD48$^-$ contour plots demonstrate that BMEC-Akt1 LT-HSCs are comparable to steady-state controls, while lung EC, brain EC, and BM EPC appeared to be in active recovery (Figure S7). While all EC transplants maintained progenitor activity following TBI, BMEC-Akt1 demonstrated the highest activity in CFU-GEMMs when compared with EC controls (Figure 7E). BMEC-Akt1 transplants also displayed improved radioprotection of the BM, spleen, and intestine when compared with EC and EPC controls (Figure 7F).

DISCUSSION

At present, it is unclear whether BMECs serve as the primary HSC niche that provides the necessary cues for maintenance of LT- HSCs in the adult BM. Recent evidence has demonstrated that EC-specific deletion of *Kitl* and *Cxcl12* results in a depletion of HSCs at steady state (Ding and Morrison, 2013; Ding et al., 2012; Greenbaum et al., 2013), while ablation of perivascular BM cells also results in significant HSC defects (Kunisaki et al., 2013; Zhou et al., 2014). However, these studies have not fully addressed the effects that cellular ablation or genetic modulation of target BM niche cells have on neighboring BM niche constituents, allowing for the possibility that reported HSC defects are indirectly due to dysfunction in untargeted niche cells. Given these limitations, we aimed to isolate BMECs and BMS cells from the BM microenvironment to explore their role in supporting HSC function, independent of other candidate BM niche cells (Calvi et al., 2003; Ding et al., 2012; Katayama et al., 2006; Kunisaki et al., 2013; Méndez-Ferrer et al., 2008, 2010; Omatsu et al., 2010; Yamazaki et al., 2011). We describe the isolation of BM-derived ECs and stroma that maintain their gene expression profiles and functional characteristics following AKT1 activation. The derivation of stable and robust primary murine BMEC-Akt1 and BMS-Akt1 cultures allowed us to interrogate their instructive functions in maintaining bona fide HSCs ex vivo, independent of exogenous serum and complex cytokine cocktails. Utilizing this system, we

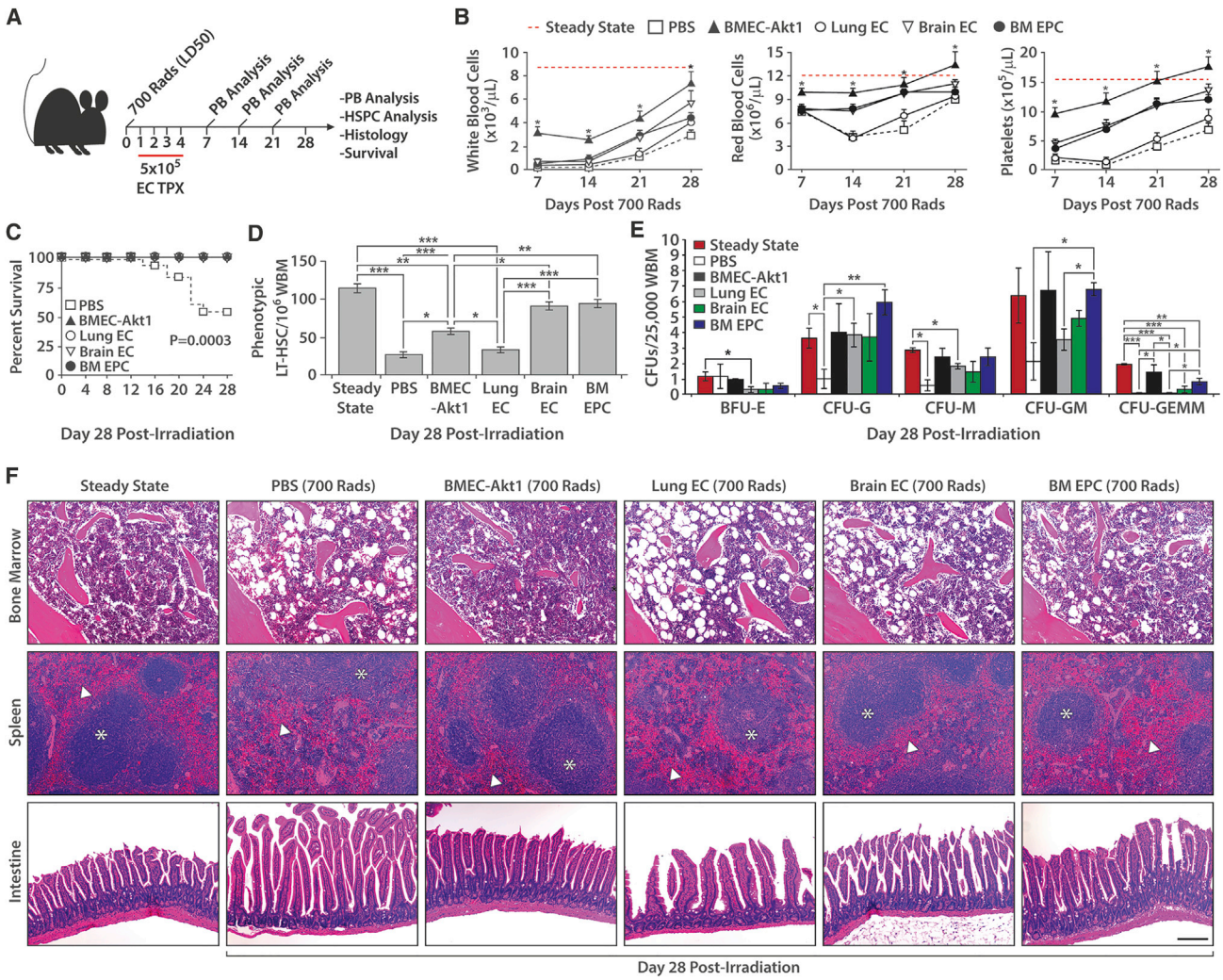

Figure 7. Niche-Specific ECs Efficiently Promote Hematopoietic Recovery Following Myeloablation

(A) C57BL/6J mice were subjected to an LD_{50} dose of TBI (700 Rads), transplanted on four successive days post-irradiation with either 5×10^5 BMEC-Akt1, 5×10^5 pulmonary artery ECs, 5×10^5 brain microvascular ECs, 5×10^5 BM EPCs, or PBS control and assayed for hematopoietic recovery.

(B) Transplantation of niche-specific BMEC-Akt1 more efficiently promotes peripheral hematopoietic recovery when compared with heterogeneous EC populations.

(C) EC transplantation mitigates radiation-induced death. All heterogeneous ECs tested promote survival following irradiation.

(D) Quantification of phenotypic LT-HSCs 28-days post-EC transplantation. LT-HSCs were quantified from WBM using LKS and $CD150^{+}CD48^{-}$ markers.

(E) Hematopoietic progenitor activity in EC transplanted mice. CFUs were assayed from $CD45^{+}$ WBM at day 28 post-irradiation.

(F) H&E-stained BM (trabecular region-femur) show cytopenia 28-days post-irradiation in EC and PBS control mice, while BMEC-Akt1 transplantations display pronounced recovery. The spleen, including both red (asterisk) and white pulp (arrowhead), and intestine also demonstrate preserved tissue morphology. n = 10 mice per cell transplant; n = 20 mice per PBS transplant. Error bars represent mean ± SEM, and significance was determined by Student's t test; $*p < 0.05$, $**p < 0.01$, $***p < 0.001$. Survival curve probability was determined using the log-rank test.

demonstrate that BMEC-Akt1 cultures, but not BMS-Akt1, are capable of supporting ex vivo cultures of LT-HSCs that achieve long-term, multilineage engraftment. While the addition of exogenous sKITL in BMEC-Akt1 co-cultures enhanced HSC engraftment, HSCs are also maintained in the absence of sKITL, suggesting that BMEC-Akt1 alone can provide sufficient cues to support repopulating HSCs ex vivo.

Given the mounting data demonstrating that HSCs reside in close proximity to the BM vascular niche, we set out to explore mechanisms that govern HSC maintenance in culture with BMEC-Akt1 and BMS-Akt1 cells. Using our co-culture system, we analyzed the differential gene expression in BMEC-Akt1 and BMS-Akt1 cells following HSPC co-culture. BMEC-Akt1 and BMS-Akt1 cells demonstrated only minor changes in known pro-HSC growth factors; however, differentially expressed chemokine/cytokine and transcription factor profiles in both BMEC-Akt1 and BMS-Akt1 cells suggest yet unappreciated reciprocal mechanisms that support HSC function. Because BMEC-Akt1, but not BMS-Akt1, were able to support bona fide LT-HSCs ex vivo, the described co-culture system can serve as a platform to identify and test growth factors that modulate LT-HSC quiescence, self-renewal, and proliferation, providing critical knowledge for the development of HSPC therapeutic applications. To further understand the intimate cross-talk between HSCs and their representative niche cells, additional transcriptional analysis of co-cultured hematopoietic cells is needed to establish a comprehensive framework outlining candidate niche-HSC interactions.

BM niche constituents, including BMECs, are susceptible to ionizing radiation and undergo non-apoptotic cell death in response to insult (Hooper et al., 2009; Kunisaki et al., 2013; Li et al., 2008). Following radiation-induced injury of BM sinusoids, HSCs relocate to the arteriole-rich endosteum vascular niche (Lo Celso et al., 2009; Xie et al., 2009). While relocation of HSCs may occur because the arteriole vascular niche is more resistant to irradiation than sinusoidal ECs, it raises the possibility that the arteriole vasculature is capable of supporting active HSPC proliferation and self-renewal, promoting hematopoietic recovery following myeloablation. This led us to examine whether BMEC-Akt1 could be used as a cellular therapy to treat hematological disorders in vivo. Using a modified transplantation protocol (Chute et al., 2007; Li et al., 2010; Salter et al., 2009), we injected BMEC-Akt1 cells following an LD_{50} dose of ionizing radiation and assessed recovery of the hematopoietic system. Cultured BMEC-Akt1 cells promoted rapid hematopoietic recovery of leukocytes, platelets, and red blood cells, with a distinct radio-protective effect on the BM HSPC compartment. Transplantation also completely mitigated radiation-induced death, while protecting the integrity of other radiosensitive tissues. Mice transplanted with BMS-Akt1 cells displayed a moderate attenuation of radiation-induced death, but did not achieve significant enhancement in hematopoietic recovery or mitigate the damage to radiosensitive tissue. Because the radio-protective effects of BMEC-Akt1 transplantations are independent of in vivo engraftment, the question remains as to how these cells transiently elicit their pro-HSPC response following myeloablation. To determine whether angiocrine factors secreted by BMEC-Akt1 cultures could enhance hematopoietic recovery following irradiation, we infused BMEC-Akt1-conditioned media. While conditioned media promote an intermediate increase in survival, they did not enhance peripheral hematopoietic recovery. The delay in hematopoietic recovery in conditioned media cohorts demonstrates that soluble factors can partially support survival, suggesting that membrane-bound factors or other cellular constituents are also important for endothelial-mediated radioprotection. Radioprotection of multiple tissues suggests a comprehensive safeguard of tissue-specific niches and resident stem cells, allowing for native regeneration following a global insult. These data provide evidence that transplantation of BMEC-Akt1 cells modulate HSPCs in vivo, promoting efficient and rapid recovery of hematopoiesis following injury. The ability to culture long-term ECs and transplant them following injury provides a unique experimental platform to test specific factors/mechanisms within endothelium that promote rapid tissue regeneration.

Previous studies have demonstrated that transplantation of allogeneic or syngeneic endothelium isolated from non-hematopoietic tissues enhance hematopoiesis following myelosuppression (Chute et al., 2007; Li et al., 2010; Montfort et al., 2002; Salter et al., 2009). We set out to test whether niche-specific BMEC-Akt1 cells would preferentially promote hematopoietic recovery following myeloablation. Compared with non-hematopoietic and secondary hematopoietic EC sources, BMEC-Akt1 was superior at promoting hematopoietic recovery following TBI and elicited a significant multiorgan radio-protective effect. These data suggest that organ-specific endothelium are more efficient in supporting the maintenance and regeneration of their tissue-resident stem cells.

It is plausible that the heterogeneous function of the vascular niche (Ding and Morrison, 2013; Ding et al., 2012; Kunisaki et al., 2013) is defined by the complex interactions between all candidate niche cells within the BM microenvironment. It is not entirely surprising that uncoupling BMECs from perivascular niche cells would allow for the maintenance of HSCs, but also require partial supplementation with sKITL. Moreover, BMS-Akt1 cells that retain MSC properties, but cannot support HSPCs ex vivo, do not rule out the possibility that the endothelial-perivascular "compound niche" is required for the maintenance of the HSC in vivo. The development of ex vivo systems that allow for the co-culture of BM niche cells is needed to elucidate cell-specific and compound niche support of HSPCs. These robust vascular and stromal platforms can also be used to examine the functional capacity of any candidate factors of interest. The described co-culture/transplantation system is not limited to HSPCs,

but can be a potentially useful platform for many tissue-specific stem cell-niche interactions.

Taken together, we have uncovered a therapeutic application for the transplantation of niche-specific BMEC-Akt1 cells following myeloablative treatment. Therapeutic transplantation of BM endothelium, with the infusion of newly discovered pro-HSPCs factors, may create a permissive microenvironment that promotes an increase in the number of engrafted HSPCs following BM transplantation, accelerating the rate of hematopoietic recovery following radiation or chemotherapeutic regimens and decreasing the morbidity and mortality associated with life-threatening pancytopenias.

EXPERIMENTAL PROCEDURES

Animals

Animal procedures were done in accordance with Weill Cornell Medical College and Institutional Animal Care and Use Committee guidelines. C57BL/6J (CD45.2) and B6.SJL-*Ptprc*^{a} *Pepc*^{b}*/BoyJ* (CD45.1) mice were obtained from Jackson Labs. *Vegfr3::YFP* mice were obtained from Jean-Leon Thomas (Calvo et al., 2011) at Yale University.

BM Endothelial and Stromal Cell Culture

BMECs were immunopurified using CD31-captured (Biolegend) magnetic beads (Life Technologies) from digested and lineage depleted (Miltenyi Biotec) adult (12 week) C57BL/6J WBM. BMS were obtained from the CD31^{-} fraction. Resulting BMEC and BMS cultures were transduced with a myristoylated-Akt1 expressing lentivirus (Kobayashi et al., 2010) and cultured on fibronectin-coated plates (Sigma-Aldrich).

Ex Vivo Hematopoietic Co-cultures

CD45.2^{+} LKS HSPCs were plated in StemSpan SFEM (StemCell Technologies) serum-free media on BMEC-Akt1/BMS-Akt1/no feeders with 50-ng/ml sKITL and cultured for 9 days. Co-cultures were supplemented with StemSpan SFEM and sKITL every 2 days and split to adjacent wells as needed. Phenotypic HSPC numbers were determined by CD45^{+} LKS quantification. To assess LT-HSC engraftment, total CD45.2^{+} co-cultured cells were transplanted with CD45.1^{+} WBM into lethally irradiated CD45.1 recipients. For secondary transplantation, WBM from primary engrafted mice was transplanted into lethally irradiated CD45.1^{+} recipients. Multilineage engraftment was determined by flow cytometry of peripheral blood.

BM Endothelial and Stromal Transplantation

Syngeneic BMEC-Akt1 and BMS-Akt1 cells were transplanted on four successive days (via retro-orbital injection) following an LD_{50} dose of TBI as previously described (Chute et al., 2007; Salter et al., 2009). C57BL/6J BMEC-Akt1 and BMS-Akt1 cells were isolated and cultured as described above. Primary C57BL/6 brain microvascular ECs, pulmonary artery ECs, and BM EPCs were obtained from Cell Biologics and cultured according to the manufacturer's suggestions. Hematopoietic recovery was monitored using an Adiva120 (Bayer Healthcare). LT-HSC frequency from WBM was determined by flow cytometry and was defined as LKS and CD150^{+}CD48^{-}.

Colony Assay

Hematopoietic progenitor activity was determined by quantifying CFUs in semisolid methylcellulose (StemCell Technologies) according to the manufacturer's protocol.

Matrigel

BMEC-Akt1 and BMS-Akt1 cells, transduced with mCherry and mCerulean expressing lentivirus, respectively (Papapetrou et al., 2009), were mixed with Matrigel (Corning) and injected subcutaneously into adult (12 week) C57BL/6J mice. Anastomosis was assessed after 14 days by intravital staining of the vasculature via retro-orbital injection of 25 μg of fluorescently conjugated VECAD antibody.

Stromal Differentiation

Subconfluent BMS-Akt1 were cultured in Osteogenic (StemCell Technologies), Adipogenic (StemCell Technologies), or Chondrogenic (Life Technologies) differentiation media for 14 days. Resulting differentiations were stained with Alizarin Red S, Oil Red O, and Toluidine Blue O or processed with Trizol (Life Technologies) according to the manufacturer's protocol. Differentiations were imaged on an Evos XL (AMG).

RNA Analysis

BMEC-Akt1 and BMS-Akt1 cells were processed using Trizol (Life Technologies) according to the manufacturer's protocol. Co-cultured feeders (CD45^{-}) were sorted into Trizol LS (Life Technologies) and processed according to the manufacturer's instructions. RNA libraries were prepared and sequenced using the TruSeq kit (Illumina) and sequenced on a HiSeq2000 (Illumina). qRT-PCR was performed using Superscript III (Life Technologies)-generated cDNA and SYBR Green (Applied Biosystems) with gene-specific primers according to the manufacturer's suggestions.

Histology and Immunhistochemistry

H&E staining of 12-μm paraffin sections was performed by Histoserv and imaged on a BX51 (Olympus) light microscope. *Vegfr3::YFP* mice were intravitally labeled with a fluorescently labeled VECAD antibody. Femurs were fixed in 4% paraformaldehyde (PFA), decalcified in 10% EDTA, and embedded in O.C.T. (VWR); 12 μm cryosections were post-stained with a SCA1 antibody. Cultured BMEC-Akt1 and BMS-Akt1 cells were fixed in 4% PFA and post-stained with antibodies as previously described (Butler et al., 2010; Poulos et al., 2013). Sections were counterstained with DAPI (Biolegend) and imaged on a LSM 710 confocal microscope (Zeiss).

Statistics

Survival curve significance was calculated using the log-rank test. Statistical significance was determined using Student's t test, and values are represented as SEM.

ACCESSION NUMBERS

The accession number for all gene expression data in this publication is NCBI GEO: GSE61636.

SUPPLEMENTAL INFORMATION

Supplemental Information includes Supplemental Experimental Procedures, seven figures, and two tables and can be found with this article online at http://dx.doi.org/10.1016/j.stemcr.2015.08.018.

AUTHOR CONTRIBUTIONS

M.G.P., M.C.G., and P.R. performed all experiments. J.M.B designed and supervised experiments. M.J.P.C., W.S., and O.E. performed in silico analysis and provided manuscript feedback. M.G.P. and J.M.B wrote the manuscript.

ACKNOWLEDGMENTS

We thank the Starr Foundation Tri-Institutional Core Facilities and the Weill Cornell Medical College's Genomics Core. J.M.B. is supported by the Ansary Stem Cell Institute; Tri-Institutional Stem Cell Initiative, American Society of Hematology Scholar Award, and American Federation of Aging Research Award. M.G.P. is supported by a Postdoctoral Tri-Institutional Stem Cell Initiative Fellowship (New York, NY). J.M.B. and M.G.P. are supported by a Sponsored Research Agreement from Angiocrine Bioscience.

Received: May 25, 2015
Revised: August 28, 2015
Accepted: August 31, 2015
Published: October 1, 2015

REFERENCES

Butler, J.M., Nolan, D.J., Vertes, E.L., Varnum-Finney, B., Kobayashi, H., Hooper, A.T., Seandel, M., Shido, K., White, I.A., Kobayashi, M., et al. (2010). Endothelial cells are essential for the self-renewal and repopulation of Notch-dependent hematopoietic stem cells. Cell Stem Cell *6*, 251–264.

Calvi, L.M., Adams, G.B., Weibrecht, K.W., Weber, J.M., Olson, D.P., Knight, M.C., Martin, R.P., Schipani, E., Divieti, P., Bringhurst, F.R., et al. (2003). Osteoblastic cells regulate the haematopoietic stem cell niche. Nature *425*, 841–846.

Calvo, C.F., Fontaine, R.H., Soueid, J., Tammela, T., Makinen, T., Alfaro-Cervello, C., Bonnaud, F., Miguez, A., Benhaim, L., Xu, Y., et al. (2011). Vascular endothelial growth factor receptor 3 directly regulates murine neurogenesis. Genes Dev. *25*, 831–844.

Chute, J.P., Muramoto, G.G., Salter, A.B., Meadows, S.K., Rickman, D.W., Chen, B., Himburg, H.A., and Chao, N.J. (2007). Transplantation of vascular endothelial cells mediates the hematopoietic recovery and survival of lethally irradiated mice. Blood *109*, 2365–2372.

Ding, L., and Morrison, S.J. (2013). Haematopoietic stem cells and early lymphoid progenitors occupy distinct bone marrow niches. Nature *495*, 231–235.

Ding, B.S., Nolan, D.J., Butler, J.M., James, D., Babazadeh, A.O., Rosenwaks, Z., Mittal, V., Kobayashi, H., Shido, K., Lyden, D., et al. (2010). Inductive angiocrine signals from sinusoidal endothelium are required for liver regeneration. Nature *468*, 310–315.

Ding, B.S., Nolan, D.J., Guo, P., Babazadeh, A.O., Cao, Z., Rosenwaks, Z., Crystal, R.G., Simons, M., Sato, T.N., Worgall, S., et al. (2011). Endothelial-derived angiocrine signals induce and sustain regenerative lung alveolarization. Cell *147*, 539–553.

Ding, L., Saunders, T.L., Enikolopov, G., and Morrison, S.J. (2012). Endothelial and perivascular cells maintain haematopoietic stem cells. Nature *481*, 457–462.

Greenbaum, A., Hsu, Y.M., Day, R.B., Schuettpelz, L.G., Christopher, M.J., Borgerding, J.N., Nagasawa, T., and Link, D.C. (2013). CXCL12 in early mesenchymal progenitors is required for haematopoietic stem-cell maintenance. Nature *495*, 227–230.

Hooper, A.T., Butler, J.M., Nolan, D.J., Kranz, A., Iida, K., Kobayashi, M., Kopp, H.G., Shido, K., Petit, I., Yanger, K., et al. (2009). Engraftment and reconstitution of hematopoiesis is dependent on VEGFR2-mediated regeneration of sinusoidal endothelial cells. Cell Stem Cell *4*, 263–274.

Katayama, Y., Battista, M., Kao, W.M., Hidalgo, A., Peired, A.J., Thomas, S.A., and Frenette, P.S. (2006). Signals from the sympathetic nervous system regulate hematopoietic stem cell egress from bone marrow. Cell *124*, 407–421.

Kiel, M.J., Yilmaz, O.H., Iwashita, T., Yilmaz, O.H., Terhorst, C., and Morrison, S.J. (2005). SLAM family receptors distinguish hematopoietic stem and progenitor cells and reveal endothelial niches for stem cells. Cell *121*, 1109–1121.

Kobayashi, H., Butler, J.M., O'Donnell, R., Kobayashi, M., Ding, B.S., Bonner, B., Chiu, V.K., Nolan, D.J., Shido, K., Benjamin, L., and Rafii, S. (2010). Angiocrine factors from Akt-activated endothelial cells balance self-renewal and differentiation of haematopoietic stem cells. Nat. Cell Biol. *12*, 1046–1056.

Kunisaki, Y., Bruns, I., Scheiermann, C., Ahmed, J., Pinho, S., Zhang, D., Mizoguchi, T., Wei, Q., Lucas, D., Ito, K., et al. (2013). Arteriolar niches maintain haematopoietic stem cell quiescence. Nature *502*, 637–643.

Li, X.M., Hu, Z., Jorgenson, M.L., Wingard, J.R., and Slayton, W.B. (2008). Bone marrow sinusoidal endothelial cells undergo nonapoptotic cell death and are replaced by proliferating sinusoidal cells in situ to maintain the vascular niche following lethal irradiation. Exp. Hematol. *36*, 1143–1156.

Li, B., Bailey, A.S., Jiang, S., Liu, B., Goldman, D.C., and Fleming, W.H. (2010). Endothelial cells mediate the regeneration of hematopoietic stem cells. Stem Cell Res. (Amst.) *4*, 17–24.

Lo Celso, C., Fleming, H.E., Wu, J.W., Zhao, C.X., Miake-Lye, S., Fujisaki, J., Côté, D., Rowe, D.W., Lin, C.P., and Scadden, D.T. (2009). Live-animal tracking of individual haematopoietic stem/progenitor cells in their niche. Nature *457*, 92–96.

Méndez-Ferrer, S., Lucas, D., Battista, M., and Frenette, P.S. (2008). Haematopoietic stem cell release is regulated by circadian oscillations. Nature *452*, 442–447.

Méndez-Ferrer, S., Michurina, T.V., Ferraro, F., Mazloom, A.R., Macarthur, B.D., Lira, S.A., Scadden, D.T., Ma'ayan, A., Enikolopov,

G.N., and Frenette, P.S. (2010). Mesenchymal and haematopoietic stem cells form a unique bone marrow niche. Nature *466*, 829–834.

Montfort, M.J., Olivares, C.R., Mulcahy, J.M., and Fleming, W.H. (2002). Adult blood vessels restore host hematopoiesis following lethal irradiation. Exp. Hematol. *30*, 950–956.

Morrison, S.J., and Scadden, D.T. (2014). The bone marrow niche for haematopoietic stem cells. Nature *505*, 327–334.

Morrison, S.J., and Spradling, A.C. (2008). Stem cells and niches: mechanisms that promote stem cell maintenance throughout life. Cell *132*, 598–611.

Nolan, D.J., Ginsberg, M., Israely, E., Palikuqi, B., Poulos, M.G., James, D., Ding, B.S., Schachterle, W., Liu, Y., Rosenwaks, Z., et al. (2013). Molecular signatures of tissue-specific microvascular endothelial cell heterogeneity in organ maintenance and regeneration. Dev. Cell *26*, 204–219.

Omatsu, Y., Sugiyama, T., Kohara, H., Kondoh, G., Fujii, N., Kohno, K., and Nagasawa, T. (2010). The essential functions of adipo-osteogenic progenitors as the hematopoietic stem and progenitor cell niche. Immunity *33*, 387–399.

Papapetrou, E.P., Tomishima, M.J., Chambers, S.M., Mica, Y., Reed, E., Menon, J., Tabar, V., Mo, Q., Studer, L., and Sadelain, M. (2009). Stoichiometric and temporal requirements of Oct4, Sox2, Klf4, and c-Myc expression for efficient human iPSC induction and differentiation. Proc. Natl. Acad. Sci. USA *106*, 12759–12764.

Poulos, M.G., Guo, P., Kofler, N.M., Pinho, S., Gutkin, M.C., Tikhonova, A., Aifantis, I., Frenette, P.S., Kitajewski, J., Rafii, S., and Butler, J.M. (2013). Endothelial Jagged-1 is necessary for homeostatic and regenerative hematopoiesis. Cell Rep. *4*, 1022–1034.

Salter, A.B., Meadows, S.K., Muramoto, G.G., Himburg, H., Doan, P., Daher, P., Russell, L., Chen, B., Chao, N.J., and Chute, J.P. (2009). Endothelial progenitor cell infusion induces hematopoietic stem cell reconstitution in vivo. Blood *113*, 2104–2107.

Sauvageau, G., Iscove, N.N., and Humphries, R.K. (2004). In vitro and in vivo expansion of hematopoietic stem cells. Oncogene *23*, 7223–7232.

Xie, Y., Yin, T., Wiegraebe, W., He, X.C., Miller, D., Stark, D., Perko, K., Alexander, R., Schwartz, J., Grindley, J.C., et al. (2009). Detection of functional haematopoietic stem cell niche using real-time imaging. Nature *457*, 97–101.

Yamazaki, S., Ema, H., Karlsson, G., Yamaguchi, T., Miyoshi, H., Shioda, S., Taketo, M.M., Karlsson, S., Iwama, A., and Nakauchi, H. (2011). Nonmyelinating Schwann cells maintain hematopoietic stem cell hibernation in the bone marrow niche. Cell *147*, 1146–1158.

Zhou, B.O., Yue, R., Murphy, M.M., Peyer, J.G., and Morrison, S.J. (2014). Leptin-receptor-expressing mesenchymal stromal cells represent the main source of bone formed by adult bone marrow. Cell Stem Cell *15*, 154–168.